Supporting Information

Biomimetic Fe(III)- Metal-Organic Framework nanosphere as a dual-modal probe for aqueous and intracellular sensing of Nicotine and its metabolite Cotinine

Arshminder Kaur Dhillon[a], Agrim Jhilta[a], Ritu Ladhi[a], Harshita Bagdwal[a], Ashi Singh[b], Rahul k. Verma[a] and Monika Singh[a*]

[a] Institute of Nano Science and Technology, Knowledge City, Sector-81, Mohali-140306, Punjab, INDIA

[b] Department of Chemistry, Indian Institute of Technology, Delhi

*Corresponding author: monika@inst.ac.in

Contents

Section	Description	Page No.
Section S1	General information and Experimental section	S-3 to S-6
Section S2	Characterization of Fe-MOF: Synthesis scheme, Microscopic image, Crystal data(Table 1.), PXRD profiles, TGA Profile, BET isotherm, FTIR, XPS spectra.(Figures S1-S6)	S-7 to S-13
Section S3	Emission spectra, Fluorescence enhancement with time, PXRD, Emission spectra and PXRD at different PH, Recyclability(Figures S7-S12), Lifetime measurements table (Table S2)	S-14 to S-14
Section S4	HOMO LUMO energy calculations and graphs, Tauc plot (Figure S 13, S14, S15, Table S3), UV-Vis spectra (S16) literature comparison (Table S4)	S-15 to S-21
Section S5	Cytotoxicity assay (S17), Cell viability images(S18-S21),	S-22 to S-24
References		S-25

Section S1: General information

Materials The reactants and solvents used in the procedure are obtained commercially from Sigma, CDH Fine Chemicals, and LobaChemei and used as purchased without any further purification. Potassium chloride (KCl) was obtained from Central Drug House (P) Ltd. Urea, glucose, and Sodium bicarbonate ($NaHCO_3$) were purchased from Tokyo Chemical Industry (India) Pvt. Ltd. α-Amylase was purchased from Sisco Research Laboratories Pvt. Ltd. (SRL) – India. Lysozyme, Creatinine, Sodium chloride (NaCl), Magnesium chloride ($MgCl_2$), Calcium chloride ($CaCl_2$) were purchased from Sigma Aldrich Chemicals Private Limited. L929 fibroblast cells and A549 lung cancer cells were procured from the National Centre for Cell Science (NCCS), Pune.

Physical Measurements FT-IR spectra were recorded on a PerkinElmer Spectrum I spectrometer with samples prepared as KBr pellets in the range of 4000-400 cm^{-1}. The solid-state (DRS) and solution-state UV-*Vis* spectra of the compound and analyte were explored by UV/Vis spectrophotometer (Shimadzu UV-2600). The morphological studies were carried out by field emission scanning electron microscopy (FESEM) on a JEOL JSM-7600F system. TGA analysis was carried out using the Perkin–Elmer Pyris 1 model on well-ground samples in a flowing nitrogen atmosphere at a heating rate of 10 °C/min. Emission spectra were recorded using a HITACHI instrument F-4700 spectrophotometer. Time-resolved lifetime decay profiles were measured using a photoluminescence Fluorolog 3-221 (Horiba Scientific) single photon counting controller. Powder X-ray diffraction analysis was carried out on a Bruker D8-Advance Eco Diffractometer using Ni-filtered Cu Kα radiation at room temperature. The data were collected over the range of $5° < 2\theta < 60°$ with a step size of 0.01°. The BET nitrogen isotherm analysis was carried out on Quantachrome ASiQwin at 300 K.

Experimental Section

Material and Methods All materials, chemicals, and detailed measurements are provided in supporting information.

Synthesis of Fe-MOF nanospheres

Scheme 1(A) illustrates the synthesis procedure of the Fe-MOF. Iron (III) chloride anhydrous (0.082 mol, 0.2 g) and Benzoic acid (0.436 mol, 0.8g) were dissolved in 15mL binary solvent ($V_{DMF}/V_{Acetonitrile}$ = 4:1) with continuous stirring for 20 minutes. This solution was subsequently placed in a Teflon-lined stainless steel vessel at 120°C for 96 hours. After cooling to room temperature, brownish-red crystals were obtained. Microscopic images of the Fe-MOF can be seen in Figure S1.

Single-Crystal X-ray Diffraction

Single-crystal X-ray diffraction data for Fe-MOF were collected using a Bruker D8 Quest diffractometer, equipped with a microfocus sealed tube molybdenum source (Mo Kα radiation, λ = 0.71073 Å) at room temperature (295 K). The sample-to-detector distance was set to 50 mm during data collection, and data reduction was performed using Apex4 software. Numerical absorption correction was applied via SADABS. The crystal structure was solved using the SHELXS-97 program and refined on F^2 by the full-matrix least-squares technique with the SHELXL software, within the Olex2 package. All non-hydrogen atoms were refined anisotropically, while hydrogen atoms were refined using the riding atom model according to the default parameters in SHELXL**.**

Photoluminescence Measurements

To perform fluorescence titration measurement, an aqueous suspension of Fe-MOF is prepared at a concentration of 2mg/2ml, using 60 mins of ultrasonic treatment. For nicotine sensing, varying concentrations of nicotine solution were meticulously introduced into the pre-prepared stock solution of 2000 µL of Fe-MOF, resulting in a final concentration ranging from 0 to 35 µM. In the selectivity experiment, major components of saliva (NaH_2PO_4, $NaHCO_3$, $CaCl_2$, $MgCl_2$, NaCl, KCl, lysozyme, and α- Amylase, 35 µL) were introduced and

corresponding emission spectra of Fe-MOF were evaluated under identical conditions. Similarly, for cotinine sensing, varying concentrations of cotinine solution were introduced into the pre-prepared stock solution of Fe-MOF, resulting in a final concentration spanning from 0 to 35 μM. In the selectivity experiments, major components of urine (creatinine, urea, glucose, KCl, and NaCl 35 μL) were added, and the corresponding emission spectra of Fe-MOF were obtained under similar conditions.

Cell viability studies

The biocompatibility of Fe-MOF was assessed using the MTT (3-[4,5-dimethylthiazol-2-yl]-2,5-diphenyltetrazolium bromide) assay. In brief, L929 fibroblast cells and A549 lung cancer cells were seeded in separate 96-well plates at a density of 1×10^4 cells per well. The L929 cells were cultured in Dulbecco's Modified Eagle Medium (DMEM), while the A549 cells were grown in Ham's F-12 Kaighn's modified medium, both supplemented with 10% fetal bovine serum (FBS) and 1% antibiotics. After incubating the cells at 37°C with 5% CO_2 for 24 hours, they were treated with various concentrations of Fe-MOF (5, 10, 20, 30, 40, 50, 100, and 200 μg/mL) in triplicate and incubated for an additional 24 hours. Following treatment, 25 μL of MTT reagent was added to the given wells, and the plates were incubated for 4 hours in the dark. The resulting MTT-formazan crystals were solubilized using 100 μL of DMSO, and the absorbance at 590 nm was measured using a Synergy H1 multimode plate reader. The % cell viability was calculated based on the absorbance values, with untreated cells serving as the control.

Cellular uptake and fluorescence imaging

A549 cells were cultured on 18 mm glass coverslips coated with 0.01% poly-L-lysine at a density of 10^5 cells per well and placed in six-well culture plates. After 24 hours of incubation, the culture medium was removed, and the cells were washed with PBS at pH 7.4.

Fe-MOF was then added to the cells and incubated for 6 hours. Following this, the cells were washed three times with PBS to remove any unbound Fe-MOF. The Fe-MOF-treated group was then exposed to nicotine and cotinine separately, while the positive control was treated with fresh medium and incubated for an additional 3 hours. After the final wash with PBS, the cells were fixed with 4% paraformaldehyde for 25 minutes at 4°C. The coverslips were mounted on glass slides with a glycerol solution and sealed with nail polish. Cell images were captured using confocal laser scanning microscopy (CLSM, LMS880NLO, Germany) with a 63× lens. The cells were visualized with an argon/krypton laser, at an excitation wavelength of 405 nm .

Section S2 : Characterization of Fe-MOF

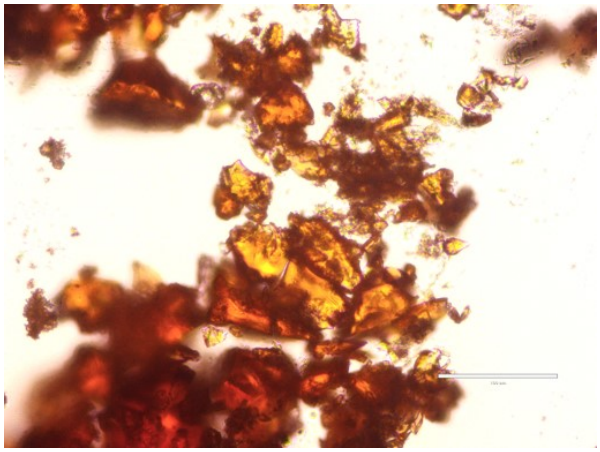

Figure S1. Microscopic image of **Fe-MOF**(Scale bar 100 μm).

Table S1 : Data obtained from the structural refinement of **Fe-MOF.**

Parameter	**MOF-1**
Formula	$[Fe_3(\mu_3\text{-}OH)(C_7O_2H_5)_6(COO)_2(H_2O).2(C_3H_7NO)]$
Formula weight, g	1119.43
T (K)	100 K
Wavelength (Å)	0.71073
Crystal system	Orthorhombic
Space Group	Pbca
a (Å)	17.1268(7)
b (Å)	20.8958(9)
c (Å)	27.5204(12)
α (°)	90
β (°)	90
γ (°)	90
V ($Å^3$)	9849.0(7)
Z	8
dcalc (gcm^{-3})	1.510
μMoKα, (cm^{-1})	0.949
R1(I>2σI)	0.0431
WR2(all)	0.1240
CCDC/CSD No.	2303436
GoF	1.068
Data(Total reflections)	12228
Restraints	0
Parameters	654
Theta range	2.085° to 28.302°

aR1 = Σ(||F0| – |FC||)/Σ|F0|; bwR2 = [Σw(|F0|2 – |FC|2)2/(Σw|F0|2) 2]1/2.

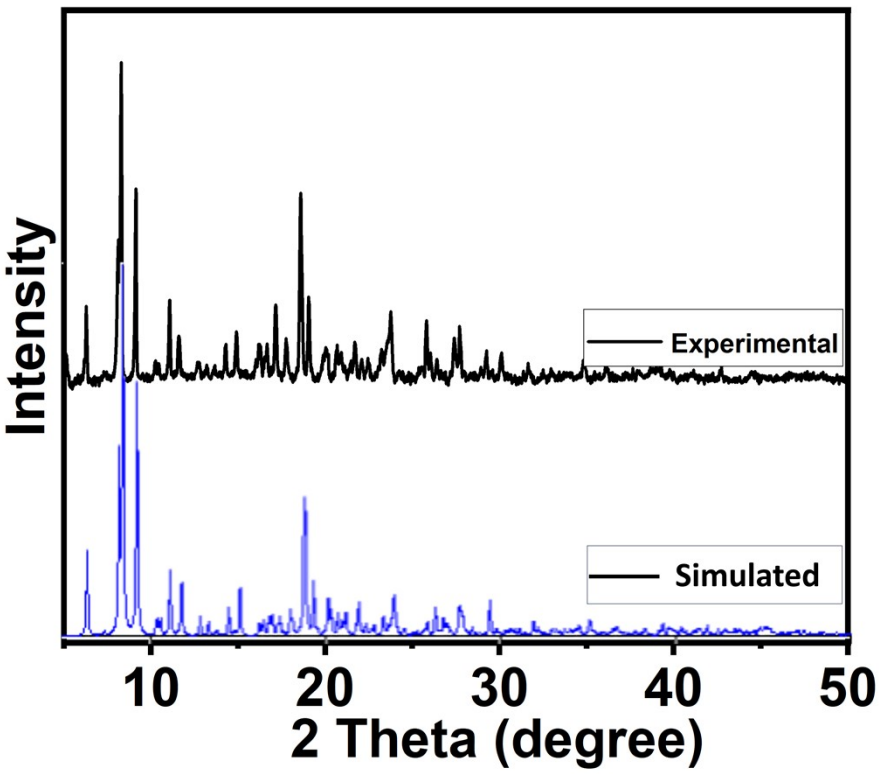

Figure S2: Simulated (blue) and the experimental (black) XRD pattern of **Fe-MOF**.

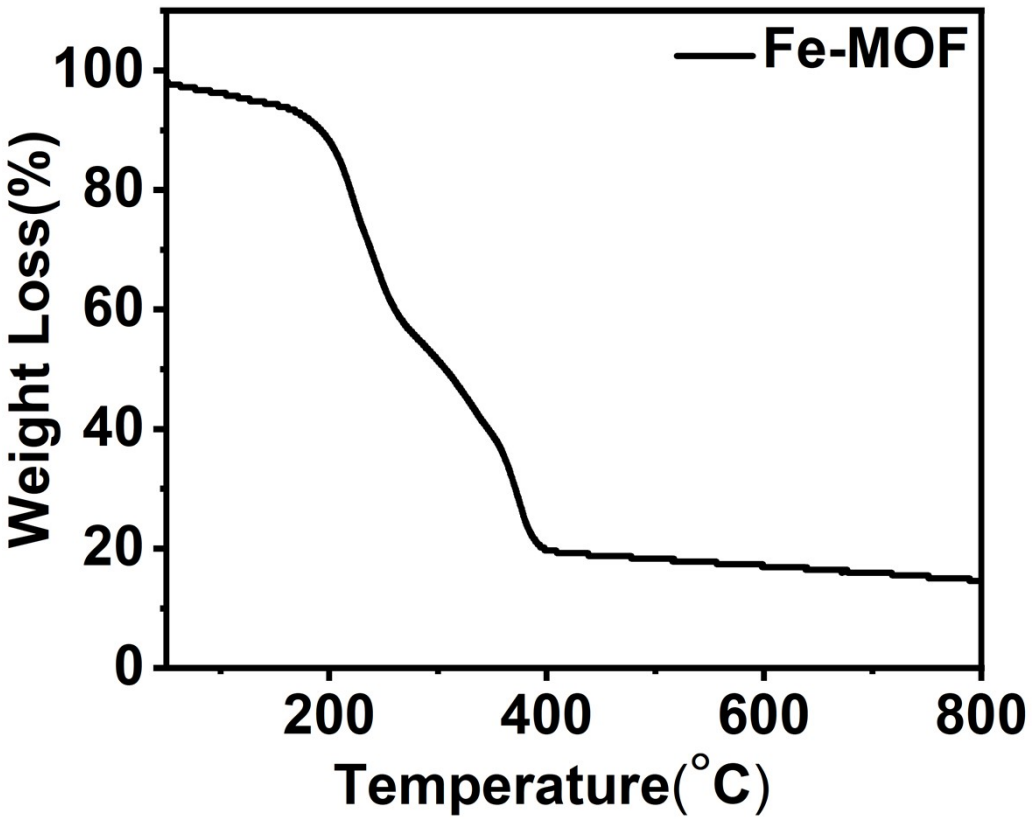

Figure S3: TGA curve of **Fe-MOF**.

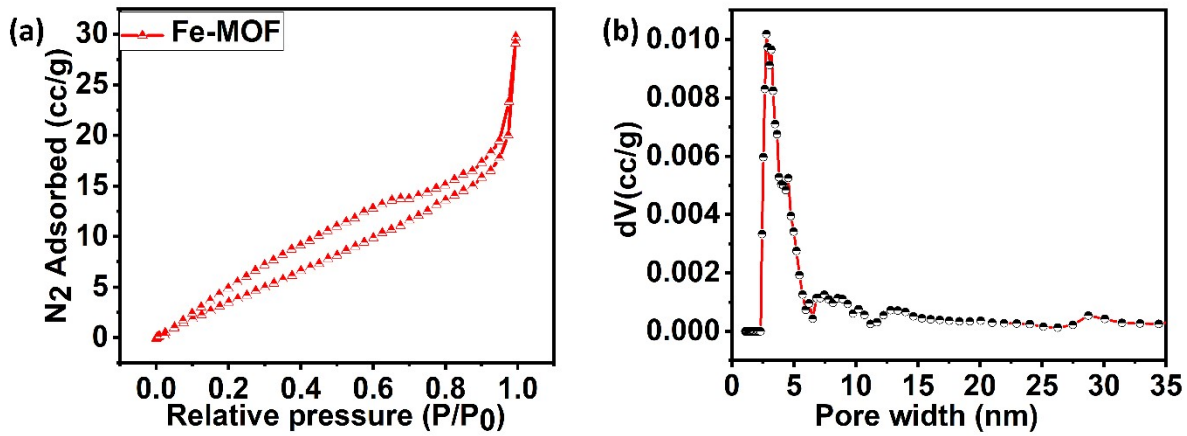

Figure S4: (a) N2 adsorption−desorption isotherms of **Fe-MOF**. (b) Pore size distribution curve of **Fe-MOF.**

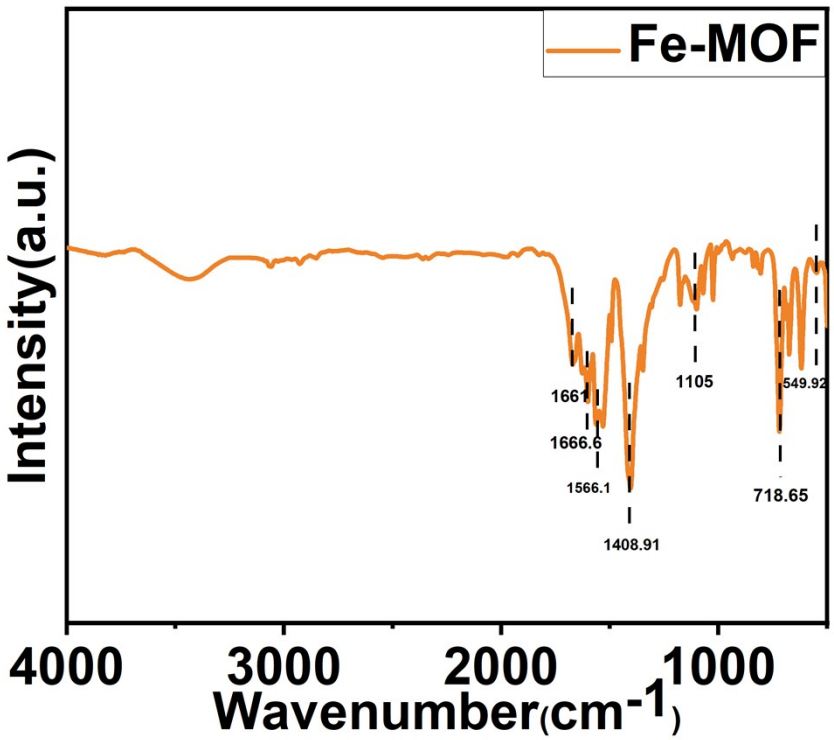

Figure S5. FT-IR of **Fe-MOF.**

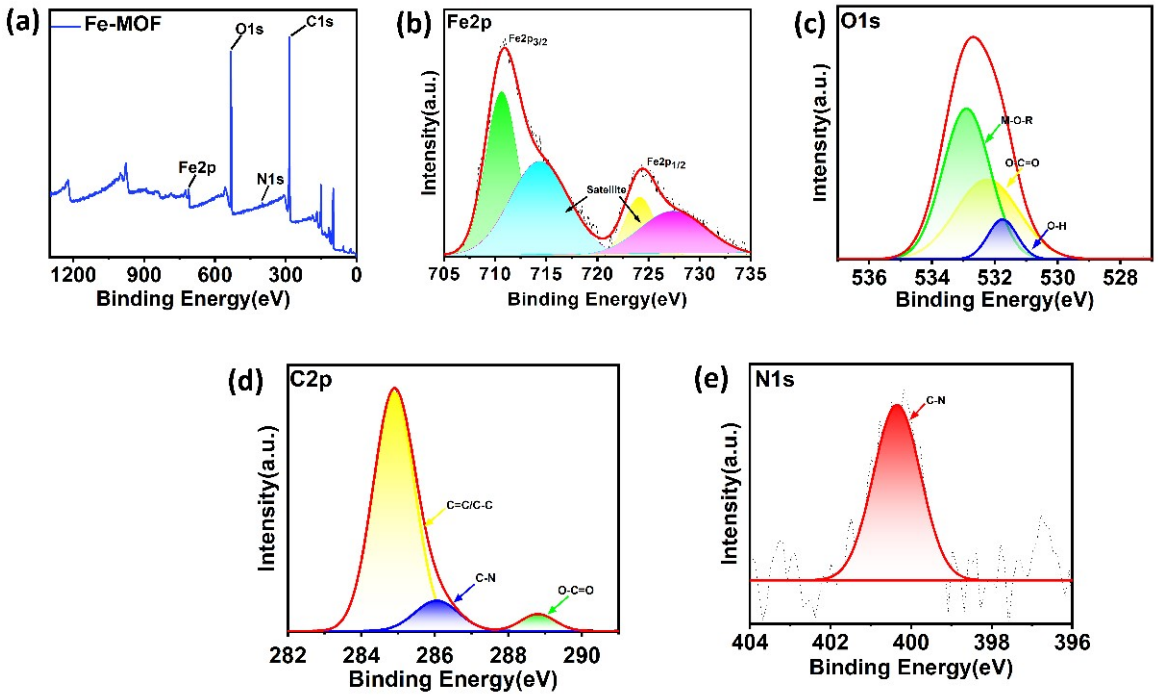

Figure S6. (a) XPS Survey spectra of **Fe-MOF**. (b-e) High-resolution spectra of Fe2p, O1s, C2p, N1s. The dotted curve is used to depict the experimental data, while the solid curve is used to demonstrate the fitting results. The peaks are allocated based on the oxidation states of certain elements and their associated linkages.

Section S3

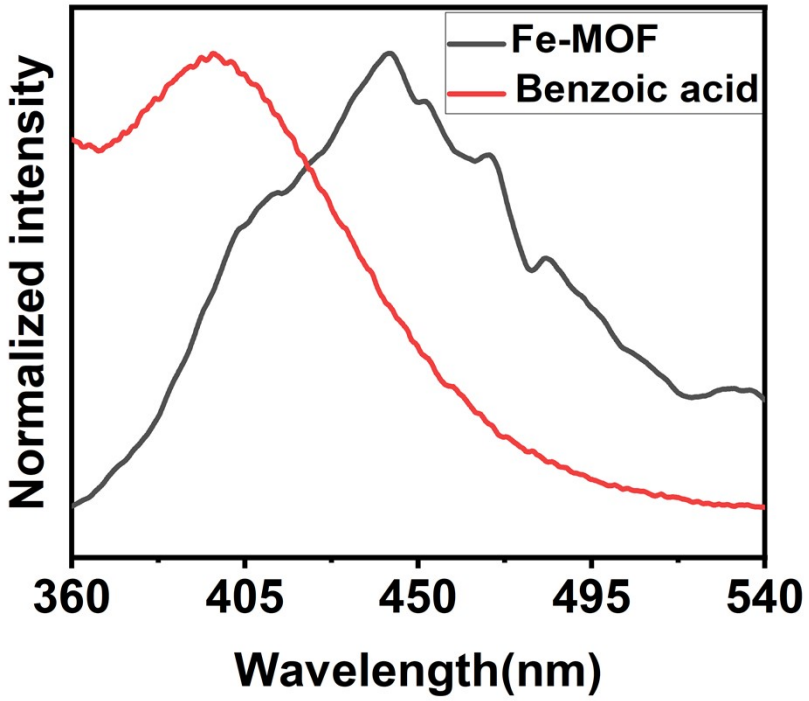

Figure S7(a). Emission spectra of **Fe-MOF** and **BA** ligand(λ_{ex}= 300nm).

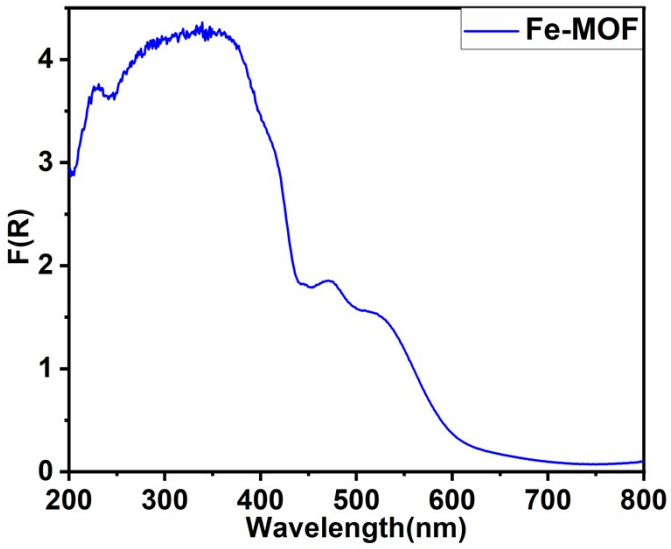

Figure S7(b). Diffuse reflectance spectra of **Fe-MOF .**

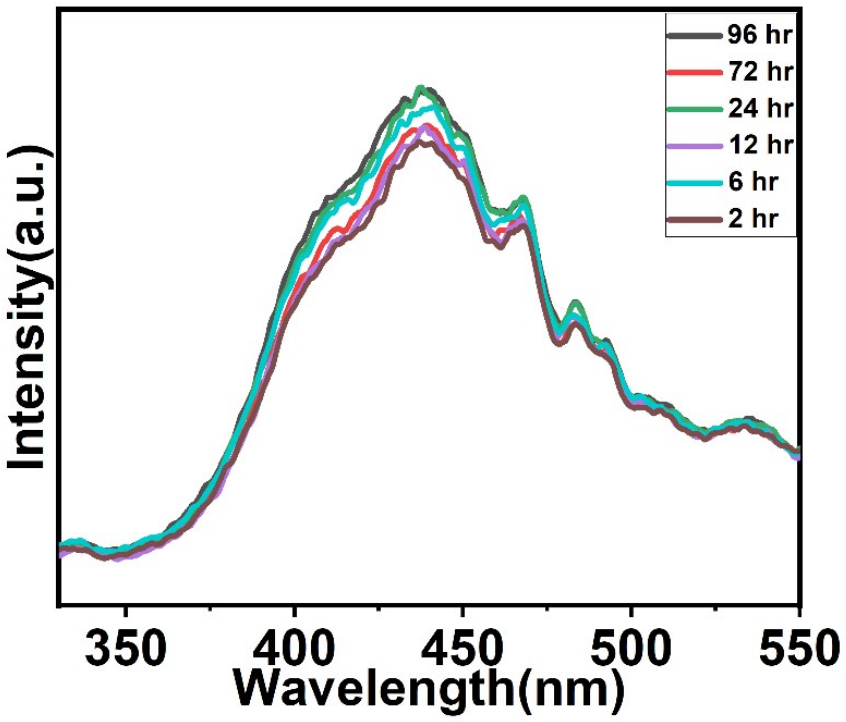

Figure S8. Evolution of fluorescent intensity of **Fe-MOF** suspension (2 mg/2mL) with various duration times under excitation at 300 nm.

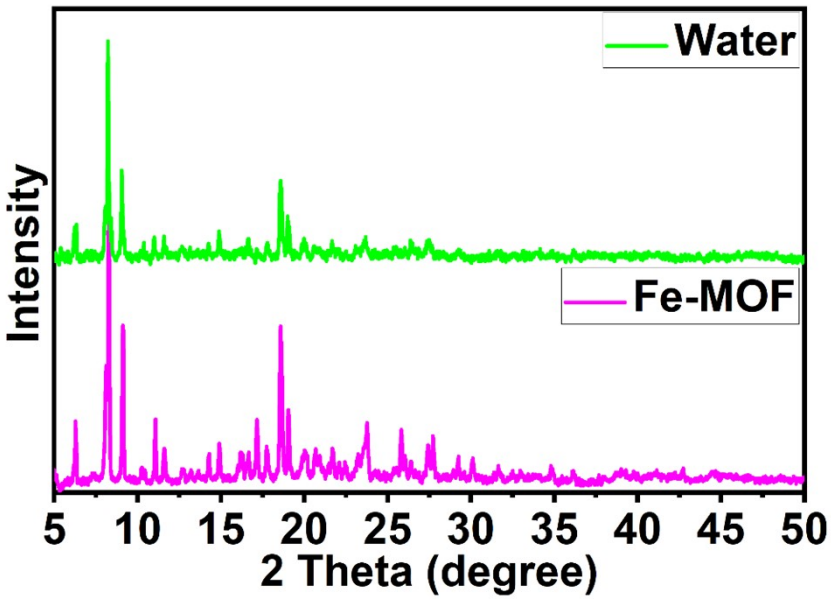

Figure S9. PXRD patterns of **Fe-MOF** immersed in water for 48 hrs.

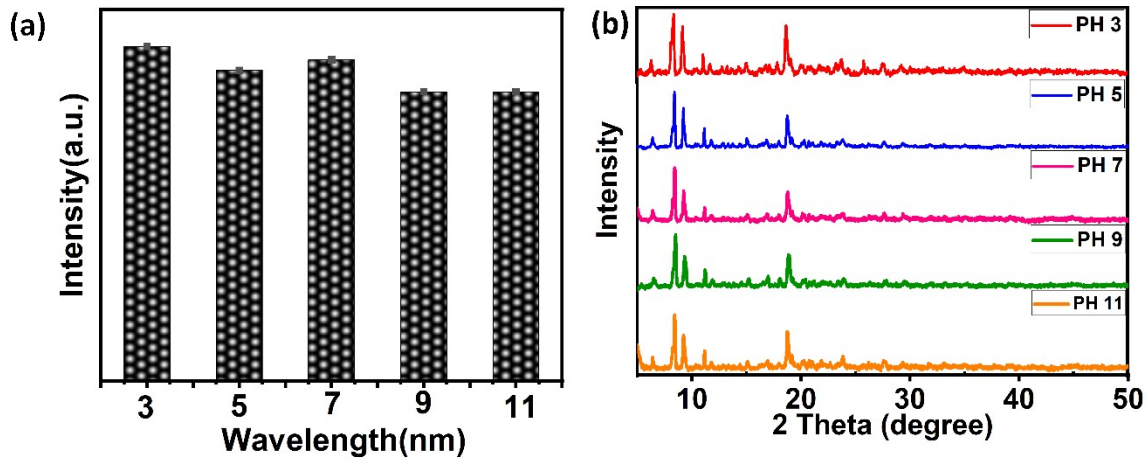

Figure S10. Effect of solution pH on the fluorescence intensity of **Fe-MOF** suspension (2 mg/mL) (b) PXRD patterns of Fe-MOF immersed in different pH solutions for 18 hrs.

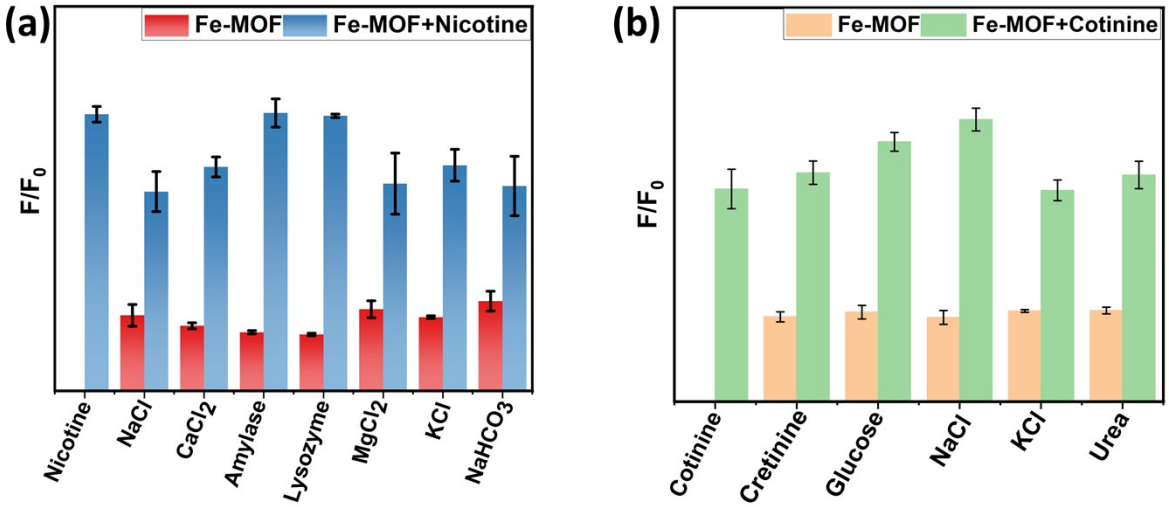

Figure S11. Competitive experiments in the absence and presence of (a) nicotine and (b) cotinine.

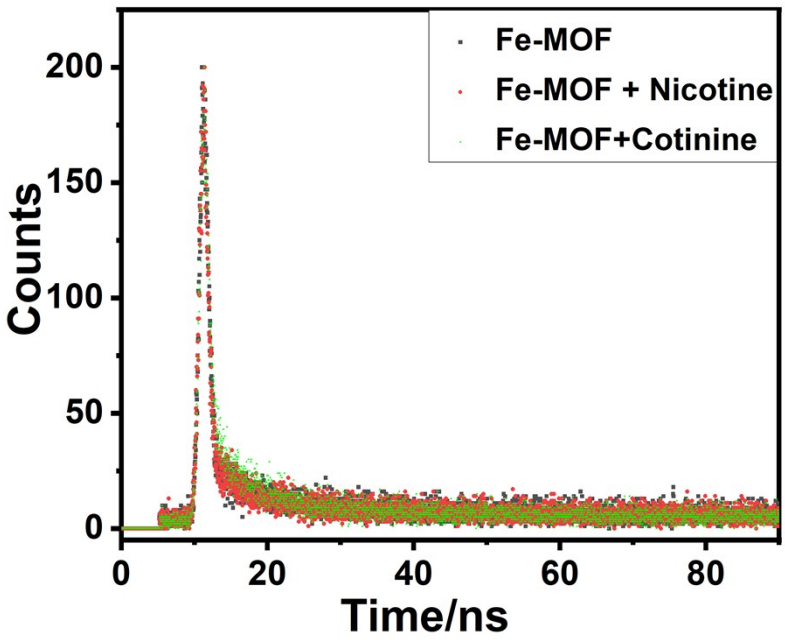

Figure S12. Lifetime decay profiles of **Fe-MOF** before and after immersing in Nicotine and Cotinine.

Table S2. Average lifetime of **Fe-MOF** before and after addition of analytes.

	Fe-MOF	**1+ Cotinine**	**1+ Nicotine**
τ_1	9.03	0.675	0.494
α_1	0.568	0.3587	10.048
τ_2	0.622	6.777	6.379
α_2	6.97	0.6413	2.319
$<\tau>$ (ns)	1.26	1.596	1.597

Section S4: HOMO LUMO energy calculations

Electrochemical measurements

To obtain HOMO and LUMO values for the **Fe-MOF**, cyclic voltammetry plots were collected for **Fe-MOF**. CV was recorded with the help of a three-electrode cell setup using Fluorine-doped Tin Oxide (FTO) as the working electrode, platinum as the counter electrode, and Ag/AgCl as a reference electrode. 0.1M tetrabutylammonium hexafluorophosphate in acetonitrile was used as an electrolyte with a scan rate of 100 mV/s[1].

Formal redox potentials (vs. AgCl/Ag), obtained by averaging the cathodic and anodic peak potentials[2].

b LUMO estimated by E_{LUMO} = -(E1 (vs. Ag/AgCl) + 4.7) (eV).

c HOMO energy of the donor estimated by $E_{HOMO} = E_{LUMO} - \Delta$.

d Energy gap estimated from the diffuse reflectance UV-vis spectrum.

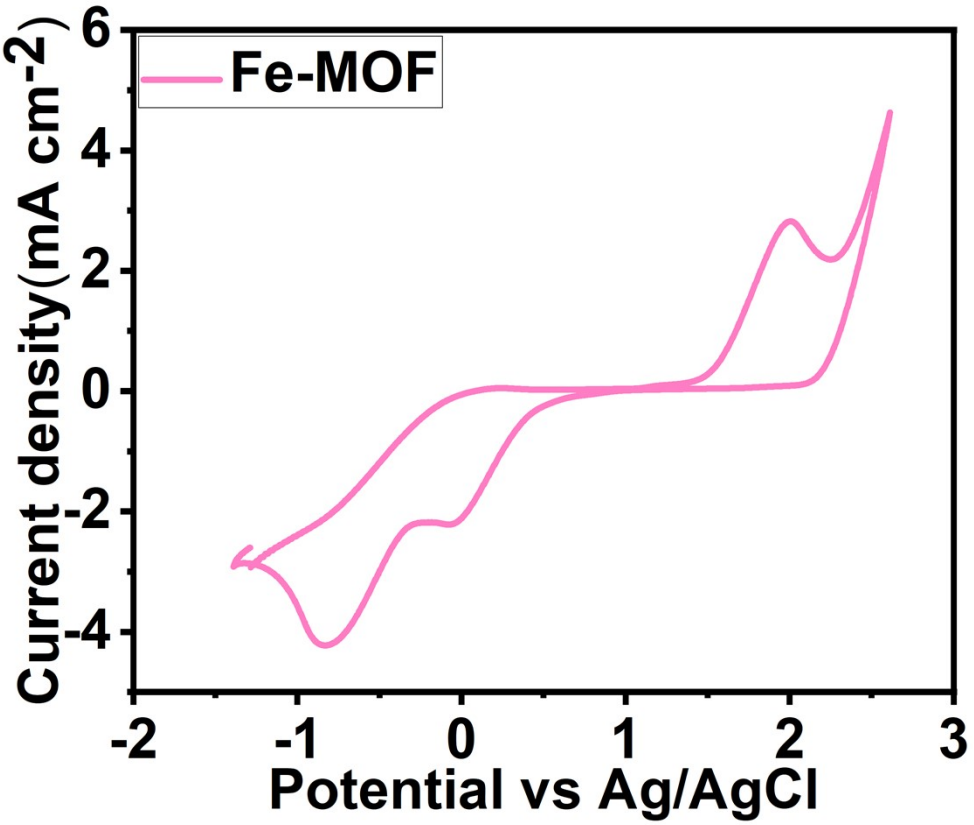

Figure S13. Cyclic voltammetry plot of **Fe-MOF**.

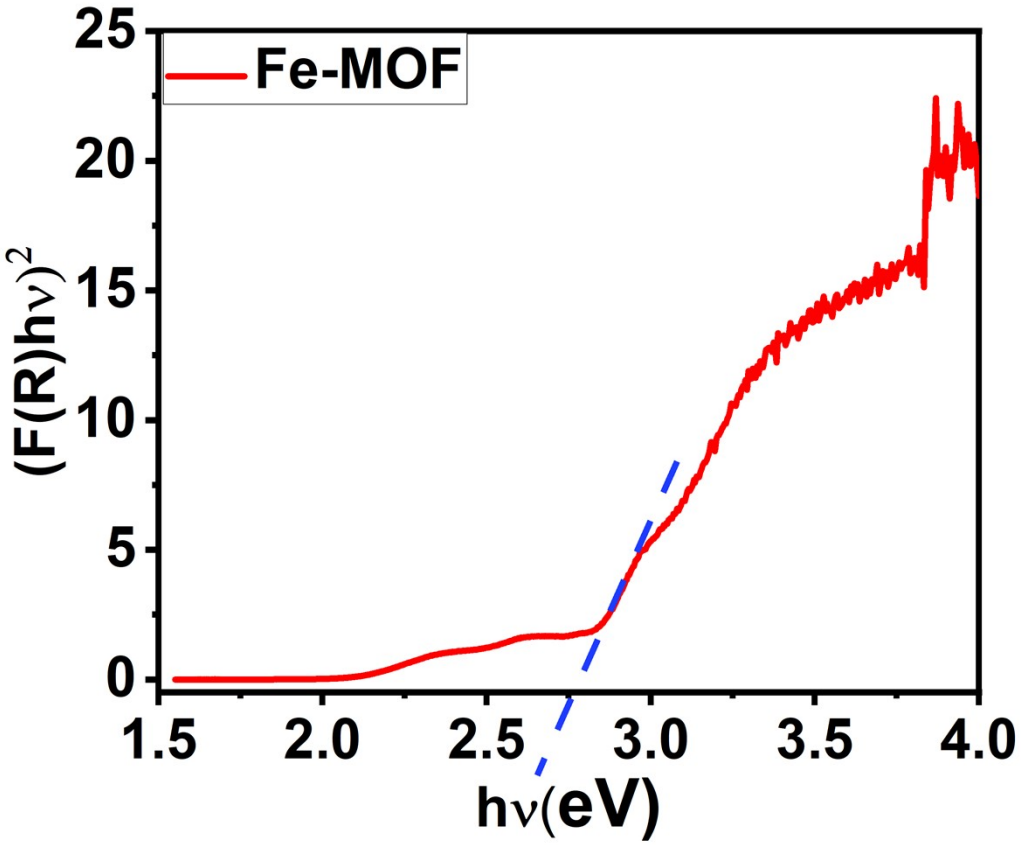

Figure S14. Tauc Plot: Band gap of **Fe-MOF.**

Optical properties concerning band gap were determined using diffused reflectance spectroscopy taking $BaSO_4$ as a reference. The band gap (Eg) was calculated by the following equation:

$(\alpha h\nu)^{1/r} = A(h\nu - Eg)^{3}$

(1) where α is the absorption coefficient, hν is discrete photon energy and A is a constant relative to the material. The absorption coefficient (α) can be related to the Kubelka-Munk function as follows: $F(R)= (1-R)^2 /2R= \alpha/S$

(2) $R=R_{sample} /R_{BaSO_4}$

(3) where F(R) is the Kubelka-Munk function, R is reflectance and S is the scattering coefficient. So, the band gap of Fe-MOF can be obtained from the plot of $(F(R)\ h\nu)^{2}$ vs hν (Tauc Plot), by extrapolating the linear regime of the resulting curves to F(R) = 0.

Herein an energy band gap of 2.75 eV for Fe-MOF was obtained (Figure S16)

Computational Methods

HOMO and LUMO energies were calculated for Nicotine and cotinine using the Gaussian 09 package and their subsequent geometry optimization was carried out at the B3LYP level of DFT[4].

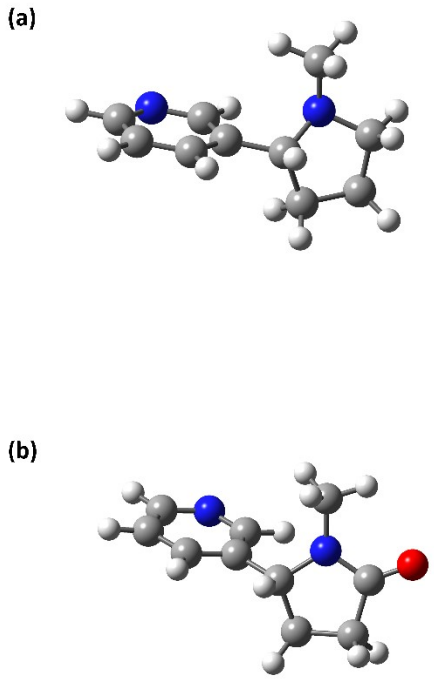

Figure S15. Optimized structure of (a) Nicotine and (b) Cotinine.

Table S3. Calculated HOMO-LUMO energies.

	E_{HOMO}(eV)	E_{LUMO}(eV)
Nicotine	-6.14	-0.91
Cotinine	-6.84	-1.28
Fe-MOF	-7.26	-4.5

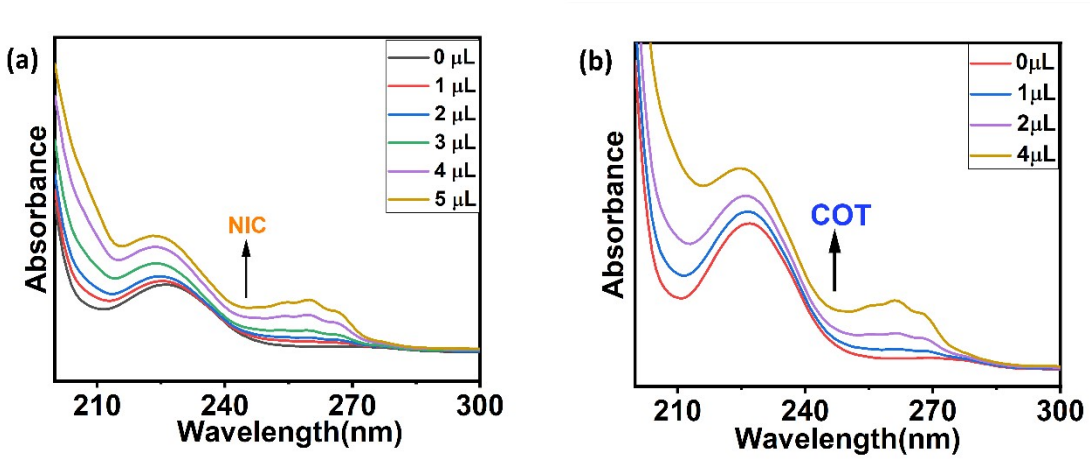

Figure S16. UV-Vis absorption spectra of Fe-MOF dispersed in aqueous solutions after adding different concentrations of (a) Nicotine and (b) Cotinine

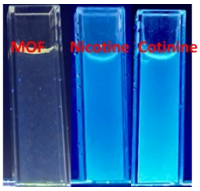

Figure S16(c) The images of **Fe-MOF** dispersed in water solutions containing Nicotine and cotinine under excitation with a 365 nm UV lamp.

Table S4 Comparative list of various fluorescent MOFs including **Fe-MOF** that have been used for sensing of Nicotine.

No.	**Metal-organic Framework**	**Analyte**	**Lumniscence type**	**Linear detection range**	**LOD (Limit of detection)**	**References**
1.	MB@UiO-66-NH2	Nicotine	Turn on	0-1000μM	0.98 μM	5
	BITSH-1,	Nicotine	Turn-off	0-1mM	20.26	1

2.	BITSH-2				62.87 µM	
3.	Fe-MOF	Nicotine , Cotinine	Turn-on	0-35µM	0.94 µM, 1.7 µM	This work

Section S5. Cellular imaging

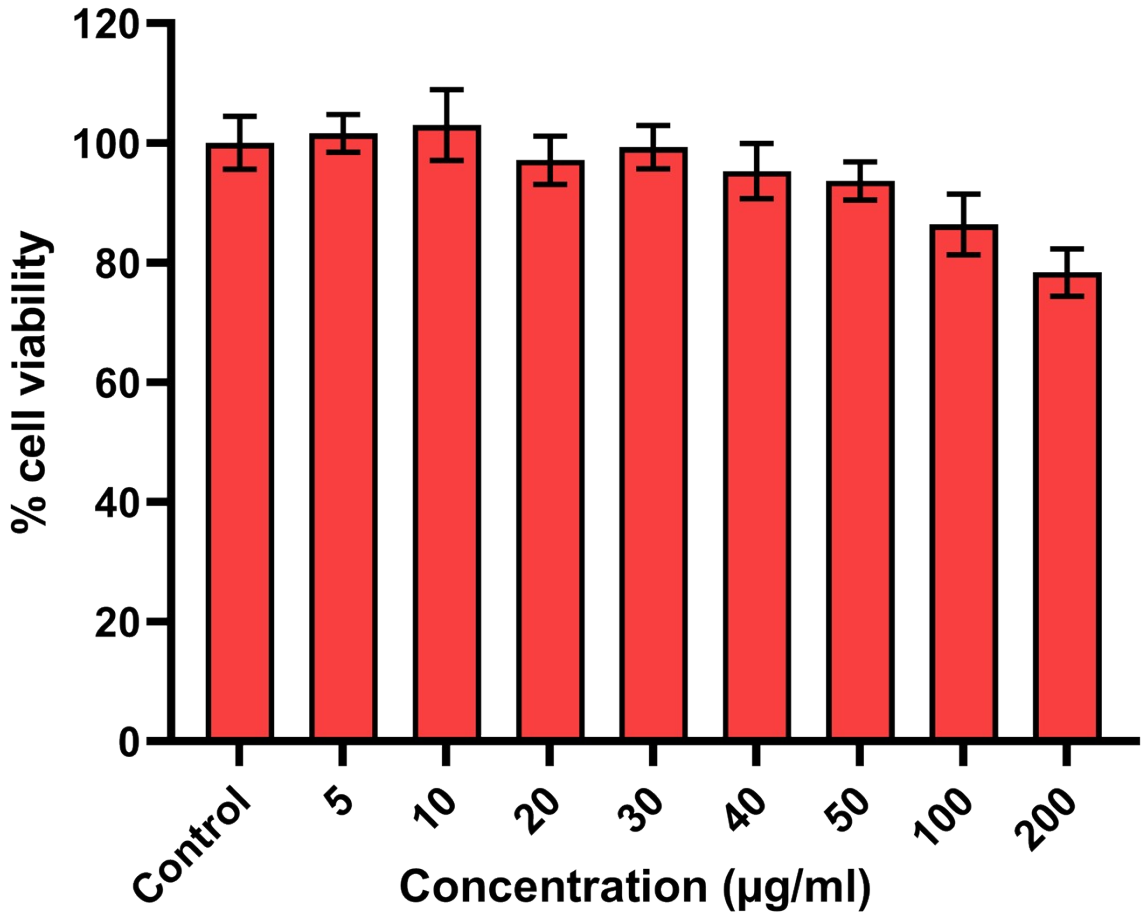

Figure S17. Cytotoxicity assay of L929 cell lines treated with different concentrations of **Fe-MOF** (red bar).

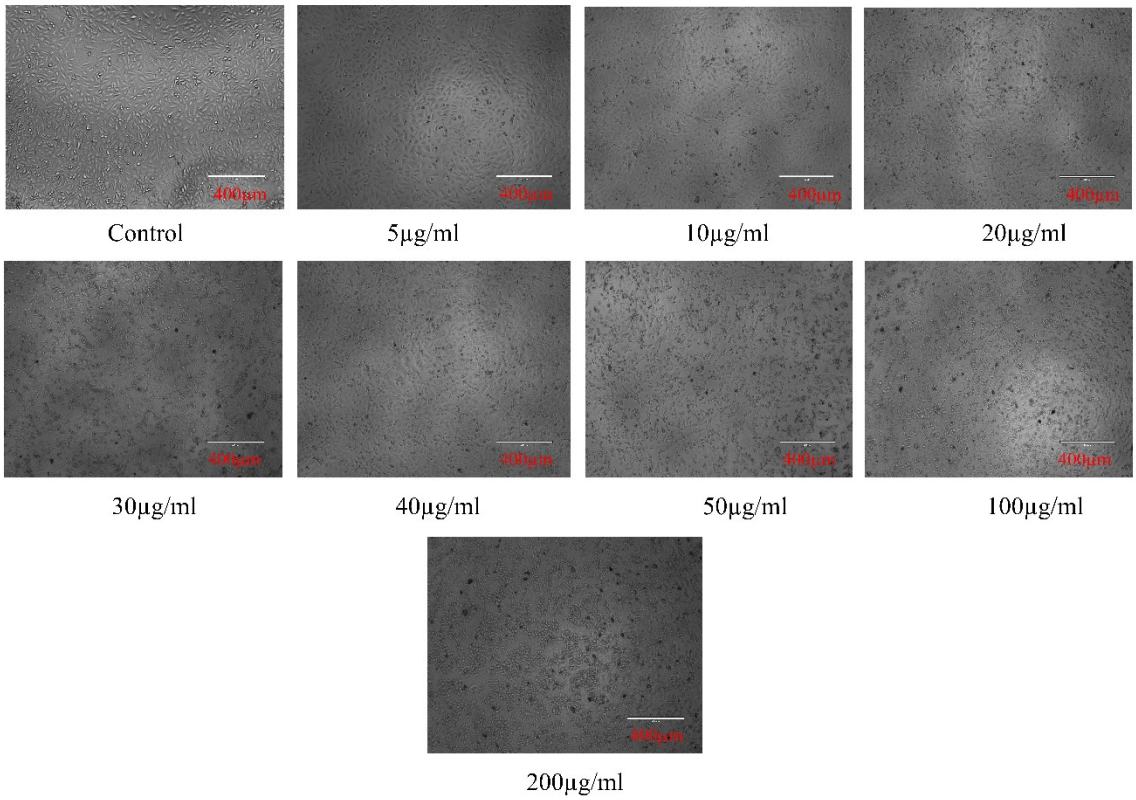

Figure S18. Bright-field image of cell viability of **Fe-MOF** in A549 cell line.

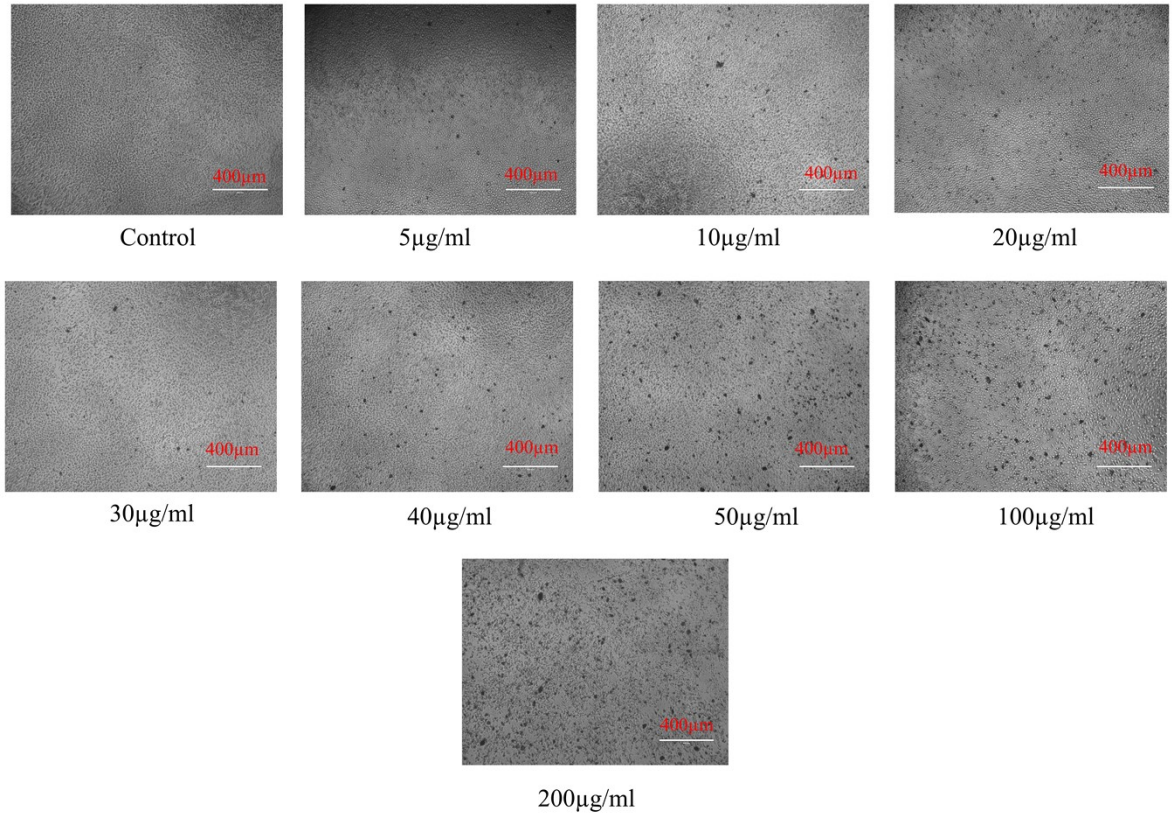

Figure S19. Bright-field image of cell viability of **Fe-MOF** in L929 cell line.

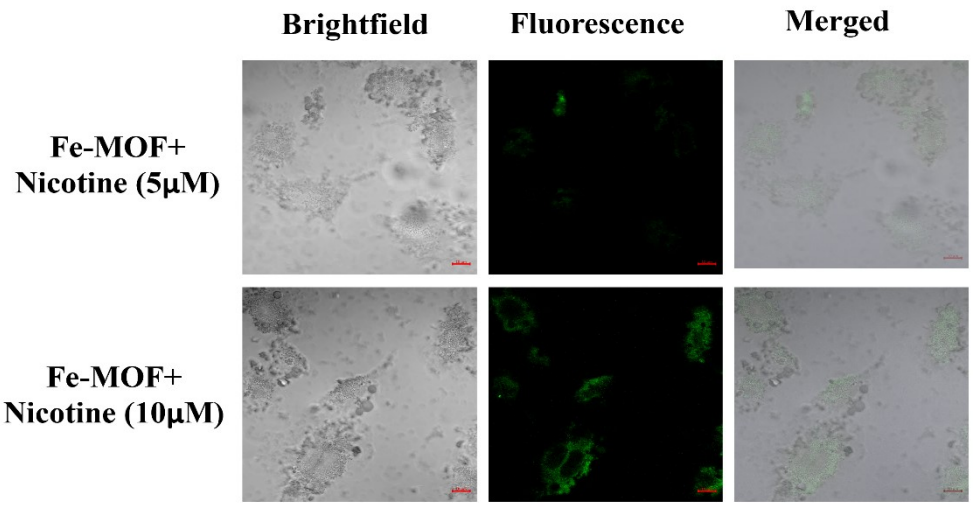

Figure S20 Confocal laser scanning microscopy images (CLSM) of Fe-MOF treated with nicotine at concentrations of 5μM and 10μM, respectively.

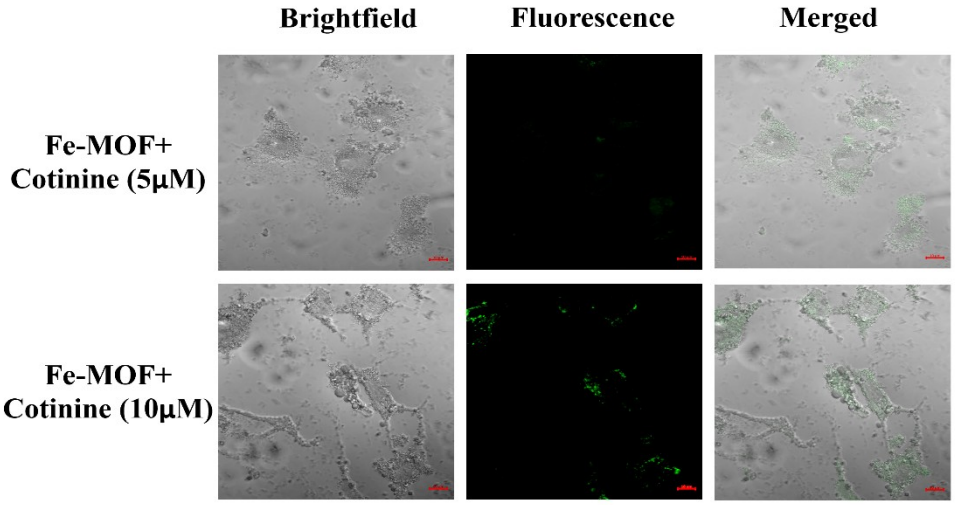

Figure S21 Confocal laser scanning microscopy images (CLSM) of Fe-MOF treated with cotinine at concentrations of 5μM and 10μM, respectively

References:

1. T. Leelasree, S. Goel and H. Aggarwal, *ACS Applied Nano Materials*, 2022, **5**, 16753-16759.
2. T. Gong, P. Li, Q. Sui, J. Chen, J. Xu and E.-Q. Gao, *Journal of Materials Chemistry A*, 2018, **6**, 9236-9244.
3. D. Rani, K. K. Bhasin and M. Singh, *ACS Materials Letters*, 2019, **2**, 9-14.
4. M. Frisch, G. Trucks, H. Schlegel, G. Scuseria, M. Robb, J. Cheeseman, G. Scalmani, V. Barone, B. Mennucci and G. Petersson, in *Gaussian 09*, Gaussian Inc Wallingford, 2009, DOI: Dalton Trans., 2015,44, 2623-2638.
5. D. Yan, Y. Lou, Y. Yang, Z. Chen, Y. Cai, Z. Guo, H. Zhan and B. Chen, *ACS applied materials interfaces*, 2019, **11**, 47253-47258.